Pramana – J. Phys. (2019) 93:81
https://doi.org/10.1007/s12043-019-1845-9

Systematic study of the α decay properties of actinides

G R SRIDHARA[1,2], H C MANJUNATHA[3,*], K N SRIDHAR[1] and H B RAMALINGAM[4]

[1]Department of Physics, Government First Grade College, Kolar 563 101, India
[2]Research and Development Centre, Bharathiar University, Coimbatore 641 046, India
[3]Department of Physics, Government College for Women, Kolar 563 101, India
[4]Department of Physics, Government Arts College, Udumalpet 642 126, India
*Corresponding author. E-mail: manjunathhc@rediffmail.com

MS received 26 March 2019; revised 7 June 2019; accepted 17 June 2019

Abstract. This work analyses the α decay properties of actinides. Geiger–Nuttall plots are presented for actinides. We have studied the competition between α decay and spontaneous fission and have identified the dominant decay mode. The results have been compared with experiments and they agree well with those of the experiments.

Keywords. Alpha decay; actinides.

PACS Nos 23.60.+e; 24.10.Eq; 27.90.+b

1. Introduction

Nuclei in the actinide region are unstable and exhibit α decay, cluster radioactivity and spontaneous fission. Dahmardeh *et al* [1] studied the influence of deformed surface diffuseness on α decay half-lives of actinides and lanthanides. Yang *et al* [2] measured the α decay properties of ^{219}Np. Three disintegration modes such as fission, cluster emission and α decay are treated in a unified manner [3]. The study of α decay properties is important in the superheavy nuclei region [4–6]. The study of α decay properties in actinides is also important in the field of materials science [7]. Many theoretical models were developed to study cluster radioactivity. Mirea *et al* [8] studied the spontaneous fission, cluster emission and α decay of ^{222}Ra using unified description. Manjunatha and Sowmya [9] studied the competition between spontaneous fission, ternary fission cluster decay and α decay in the superheavy nuclei of $Z = 126$. Silişteanu and Budaca [10] studied the α decay properties of the superheavy nuclei region. In this work, we have studied the α decay properties of actinides. This paper is organised into three sections: in §2, we have explained the methodology of calculation of α decay half-lives. In §3, we have explained the results of α decay half-lives of actinides.

2. Theory

The α decay half-life $T_{1/2}$ is related to the decay width Γ by [11,12]

$$T_{1/2} = \frac{h \times \ln 2}{2\pi \times \Gamma}, \tag{1}$$

$$\Gamma = \frac{h}{2\pi} \times \nu S_\alpha P(E) = \frac{h}{2\pi}\xi P(E), \tag{2}$$

where ν is the assault frequency of α-particle on the barrier and S_α is the spectroscopic or preformation factor of α-particle inside the parent nucleus. ξ is parameterised as [11,12]

$$\xi = \left(6.1814 + 0.29A^{-1/6}\right) \times 10^{19}\ \mathrm{s}^{-1}, \tag{3}$$

P is the barrier penetration probability and it is derived from the Wentzel–Kramers–Brillouin (WKB) approximation,

$$P(E) = \exp\left[-2\int_{R_{\rm in}}^{R_{\rm out}} \sqrt{\frac{8\pi^2 \times \mu}{h^2}(V(R) - Q_\alpha)}\, \mathrm{d}R\right], \tag{4}$$

where $V(R)$ is the potential barrier, Q_α is the α decay energy, $\mu = (M_\alpha M_{\rm d})/(M_\alpha + M_{\rm d})$ is the reduced mass

Published online: 28 August 2019

Table 1. Competition between spontaneous fission and α decay.

Nuclei	Q (MeV)	Penetration probability	$\log(T_{1/2})$				$\log(T_{sf})$	Decay modes
			Expt.	Present work	UDL	UNIV		
^{210}Ac	8.327	2.73×10^{-19}	–	−2.83	−3.07	−3.16	−4.95	SF
^{211}Ac	8.166	3.03×10^{-19}	–	−2.40	−2.61	−2.71	−1.40	α
^{212}Ac	8.003	2.00×10^{-19}	–	−1.96	−2.13	−2.24	1.98	α
^{213}Ac	7.838	1.99×10^{-19}	–	−1.51	−1.64	−1.75	5.17	α
^{214}Ac	7.672	1.13×10^{-19}	–	−1.02	−1.11	−1.24	8.19	α
^{215}Ac	7.504	1.13×10^{-19}	–	−0.52	−0.57	−0.70	11.03	α
^{216}Ac	7.334	1.41×10^{-15}	−3.36	−3.52	−3.59	−3.63	13.68	α
^{217}Ac	7.163	3.90×10^{-14}	−7.16	−7.50	−7.65	−7.73	16.16	α
^{218}Ac	6.990	3.33×10^{-15}	−5.91	−6.19	−6.31	−6.38	18.46	α
^{219}Ac	6.816	1.26×10^{-16}	−4.54	−4.76	−4.85	−4.90	20.58	α
^{220}Ac	6.641	2.05×10^{-16}	−1.58	−1.66	−1.69	−1.71	22.53	α
^{221}Ac	6.464	1.40×10^{-17}	−1.28	−1.34	−1.37	−1.38	24.29	α
^{222}Ac	6.285	6.16×10^{-20}	−1.90	−1.99	−2.03	−2.05	25.87	α
^{223}Ac	6.105	1.60×10^{-19}	5.91	6.19	6.31	6.38	27.28	α
^{224}Ac	5.923	2.20×10^{-21}	–	5.24	5.69	5.57	28.51	α
^{225}Ac	5.738	5.61×10^{-22}	–	6.08	6.60	6.48	29.55	α
^{226}Ac	5.551	1.24×10^{-22}	–	6.96	7.56	7.45	30.42	α
^{227}Ac	5.360	2.80×10^{-23}	–	7.91	8.59	8.50	31.12	α
^{228}Ac	5.165	1.44×10^{-23}	–	8.94	9.71	9.64	31.63	α
^{229}Ac	4.965	7.52×10^{-24}	–	10.06	10.92	10.87	31.96	α
^{230}Ac	4.761	6.32×10^{-24}	–	11.27	12.24	12.22	32.12	α
^{231}Ac	4.552	5.56×10^{-25}	–	12.60	13.68	13.70	32.09	α
^{232}Ac	4.340	8.65×10^{-26}	–	14.04	15.25	15.32	31.89	α
^{233}Ac	4.125	1.32×10^{-25}	–	15.62	16.96	17.08	31.51	α
^{234}Ac	3.911	2.19×10^{-26}	–	17.32	18.81	18.98	30.95	α
^{235}Ac	3.701	1.69×10^{-26}	–	19.13	20.78	21.02	30.22	α
^{236}Ac	3.498	7.51×10^{-27}	–	21.04	22.85	23.17	29.30	α
^{237}Ac	3.305	5.52×10^{-27}	–	23.01	24.99	25.39	28.21	α
^{238}Ac	3.125	3.32×10^{-27}	–	25.01	27.16	27.65	26.94	α
^{200}Th	10.358	6.75×10^{-15}	–	−6.97	−7.57	−7.48	−64.60	SF
^{201}Th	10.227	1.32×10^{-15}	–	−6.73	−7.31	−7.24	−58.88	SF
^{202}Th	10.093	2.81×10^{-16}	–	−6.48	−7.04	−6.98	−53.34	SF
^{203}Th	9.956	1.61×10^{-16}	–	−6.22	−6.75	−6.71	−47.99	SF
^{204}Th	9.817	4.66×10^{-17}	–	−5.94	−6.45	−6.42	−42.81	SF
^{205}Th	9.675	1.82×10^{-17}	–	−5.65	−6.14	−6.13	−37.81	SF
^{206}Th	9.531	3.78×10^{-18}	–	−5.36	−5.82	−5.82	−32.99	SF
^{207}Th	9.384	1.12×10^{-18}	–	−5.05	−5.48	−5.49	−28.35	SF
^{208}Th	9.236	3.54×10^{-19}	−2.77	−2.90	−2.96	−2.99	−23.89	SF
^{209}Th	9.085	1.69×10^{-19}	−2.60	−2.72	−2.78	−2.81	−19.61	SF
^{210}Th	8.932	2.74×10^{-19}	−1.80	−1.89	−1.92	−1.94	−15.51	SF
^{211}Th	8.776	6.08×10^{-18}	−1.43	−1.50	−1.53	−1.54	−11.59	SF
^{212}Th	8.619	6.49×10^{-19}	−1.50	−1.57	−1.60	−1.62	−7.85	SF
^{213}Th	8.461	4.56×10^{-18}	−0.84	−0.88	−0.90	−0.91	−4.29	SF
^{214}Th	8.300	1.30×10^{-19}	−1.06	−1.11	−1.13	−1.14	−0.91	α
^{215}Th	8.137	2.17×10^{-19}	0.08	0.08	0.09	0.09	2.29	α
^{216}Th	7.973	3.98×10^{-19}	−1.59	−1.67	−1.70	−1.72	5.32	α
^{217}Th	7.807	1.87×10^{-15}	−3.60	−3.77	−3.84	−3.89	8.16	α
^{218}Th	7.640	1.84×10^{-14}	−6.91	−7.24	−7.38	−7.46	10.83	α
^{219}Th	7.471	3.36×10^{-15}	−5.98	−6.33	−6.39	−6.45	13.31	α
^{220}Th	7.301	1.24×10^{-16}	−5.01	−5.30	−5.35	−5.41	15.62	α

Table 1. *Continued.*

Nuclei	Q (MeV)	Penetration probability	$\log(T_{1/2})$				$\log(T_{sf})$	Decay modes
			Expt.	Present work	UDL	UNIV		
^{221}Th	7.129	2.08×10^{-17}	−2.76	−2.92	−2.95	−2.98	17.75	α
^{222}Th	6.956	1.91×10^{-18}	−2.65	−2.80	−2.83	−2.86	19.70	α
^{223}Th	6.781	3.12×10^{-18}	−0.22	−0.23	−0.23	−0.24	21.47	α
^{224}Th	6.604	6.55×10^{-20}	0.02	0.02	0.02	0.02	23.06	α
^{225}Th	6.426	1.24×10^{-20}	2.72	2.88	2.90	2.94	24.48	α
^{226}Th	6.244	2.15×10^{-21}	3.26	3.45	3.48	3.52	25.71	α
^{227}Th	6.060	7.07×10^{-22}	6.21	6.57	6.63	6.70	26.77	α
^{228}Th	5.873	8.34×10^{-23}	7.78	8.23	8.31	8.40	27.64	α
^{229}Th	5.681	3.57×10^{-23}	11.40	12.06	12.17	12.30	28.34	α
^{230}Th	5.485	6.68×10^{-24}	12.38	13.10	13.22	13.36	28.86	α
^{231}Th	5.284	9.38×10^{-25}	–	8.73	9.48	9.40	29.20	α
^{232}Th	5.078	5.99×10^{-25}	17.65	18.67	19.24	19.34	29.36	α
^{233}Th	4.868	1.58×10^{-25}	–	11.07	12.02	11.99	29.35	α
^{234}Th	4.657	2.40×10^{-26}	–	12.38	13.45	13.46	29.15	α
^{235}Th	4.446	1.97×10^{-26}	–	13.78	14.97	15.02	28.78	α
^{236}Th	4.239	4.37×10^{-26}	–	15.27	16.58	16.68	28.23	α
^{200}Pa	10.873	3.37×10^{-14}	–	−7.65	−8.31	−8.18	−79.52	SF
^{201}Pa	10.749	1.04×10^{-15}	–	−7.44	−8.08	−7.96	−73.44	SF
^{202}Pa	10.623	7.19×10^{-14}	–	−7.22	−7.84	−7.74	−67.53	SF
^{203}Pa	10.494	3.26×10^{-16}	–	−6.99	−7.59	−7.50	−61.80	SF
^{204}Pa	10.362	1.84×10^{-17}	–	−6.75	−7.33	−7.26	−56.26	SF
^{205}Pa	10.227	2.40×10^{-17}	–	−6.50	−7.06	−7.00	−50.89	SF
^{206}Pa	10.090	9.34×10^{-18}	–	−6.24	−6.78	−6.73	−45.71	SF
^{207}Pa	9.950	9.29×10^{-18}	–	−5.97	−6.48	−6.45	−40.70	SF
^{208}Pa	9.808	2.67×10^{-18}	–	−5.68	−6.17	−6.15	−35.88	SF
^{209}Pa	9.664	8.37×10^{-19}	–	−5.39	−5.85	−5.84	−31.23	SF
^{210}Pa	9.517	1.70×10^{-22}	–	−5.08	−5.52	−5.52	−26.76	SF
^{211}Pa	9.368	5.52×10^{-18}	−6.52	−6.90	−7.11	−7.15	−22.48	SF
^{212}Pa	9.218	4.18×10^{-19}	−2.29	−2.42	−2.50	−2.51	−18.37	SF
^{213}Pa	9.065	5.33×10^{-17}	−2.28	−2.41	−2.49	−2.50	−14.44	SF
^{214}Pa	8.910	8.88×10^{-19}	−1.77	−1.87	−1.93	−1.94	−10.69	SF
^{215}Pa	8.753	2.55×10^{-18}	−1.85	−1.96	−2.02	−2.03	−7.12	SF
^{216}Pa	8.595	5.04×10^{-19}	−0.82	−0.87	−0.89	−0.90	−3.73	SF
^{217}Pa	8.435	4.37×10^{-18}	−2.42	−2.56	−2.64	−2.65	−0.52	α
^{218}Pa	8.273	6.36×10^{-15}	−3.48	−3.69	−3.79	−3.81	2.51	α
^{219}Pa	8.109	3.00×10^{-14}	−7.28	−7.71	−7.94	−7.98	5.36	α
^{220}Pa	7.944	8.83×10^{-15}	−6.11	−6.47	−6.66	−6.70	8.03	α
^{221}Pa	7.778	1.24×10^{-13}	–	−0.73	−0.79	−0.92	10.53	α
^{222}Pa	7.609	1.46×10^{-17}	–	−0.22	−0.24	−0.38	12.84	α
^{223}Pa	7.440	5.71×10^{-17}	–	0.30	0.33	0.19	14.98	α
^{224}Pa	7.268	1.33×10^{-19}	–	0.86	0.93	0.78	16.93	α
^{225}Pa	7.095	4.74×10^{-20}	–	1.44	1.56	1.40	18.71	α
^{226}Pa	6.920	8.93×10^{-21}	2.03	2.15	2.21	2.22	20.31	α
^{227}Pa	6.742	1.98×10^{-21}	3.36	3.56	3.66	3.68	21.73	α
^{228}Pa	6.561	5.66×10^{-22}	–	3.36	3.65	3.50	22.97	α
^{229}Pa	6.377	1.43×10^{-22}	–	4.09	4.44	4.29	24.04	α
^{230}Pa	6.189	3.92×10^{-23}	–	4.86	5.28	5.13	24.92	α
^{231}Pa	5.996	1.50×10^{-23}	12.01	12.72	13.11	13.16	25.63	α
^{232}Pa	5.798	2.05×10^{-24}	–	6.58	7.15	7.03	26.15	α
^{233}Pa	5.595	4.82×10^{-25}	–	7.56	8.21	8.09	26.50	α

Table 1. *Continued.*

Nuclei	Q (MeV)	Penetration probability	$\log(T_{1/2})$				$\log(T_{\mathrm{sf}})$	Decay modes
			Expt.	Present work	UDL	UNIV		
^{234}Pa	5.389	7.83×10^{-26}	–	8.60	9.34	9.25	26.67	α
^{235}Pa	5.181	2.87×10^{-25}	–	9.71	10.55	10.48	26.66	α
^{236}Pa	4.973	3.23×10^{-26}	–	10.90	11.84	11.80	26.48	α
^{237}Pa	4.769	4.05×10^{-26}	–	12.15	13.19	13.18	26.11	α
^{238}Pa	4.571	1.17×10^{-26}	–	13.42	14.57	14.60	25.57	α
^{239}Pa	4.384	3.17×10^{-26}	–	14.71	15.97	16.03	24.85	α
^{240}Pa	4.210	3.02×10^{-26}	–	15.99	17.36	17.46	23.95	α
^{210}U	10.084	1.58×10^{-18}	–	−5.99	−6.51	−6.47	−38.69	SF
^{211}U	9.942	2.08×10^{-17}	–	−5.71	−6.20	−6.18	−34.04	SF
^{212}U	9.797	9.24×10^{-19}	–	−5.41	−5.88	−5.87	−29.57	SF
^{213}U	9.651	2.47×10^{-17}	–	−5.11	−5.55	−5.56	−25.27	SF
^{214}U	9.502	4.27×10^{-18}	–	−4.80	−5.21	−5.23	−21.16	SF
^{215}U	9.351	1.76×10^{-18}	−3.15	−3.34	−3.44	−3.45	−17.22	SF
^{216}U	9.198	7.28×10^{-19}	−2.35	−2.49	−2.56	−2.58	−13.47	SF
^{217}U	9.044	2.53×10^{-19}	−1.80	−1.91	−1.96	−1.97	−9.89	SF
^{218}U	8.888	1.06×10^{-18}	–	−3.40	−3.69	−3.75	−6.49	SF
^{219}U	8.730	2.17×10^{-16}	−4.38	−4.64	−4.78	−4.80	−3.27	α
^{220}U	8.570	2.32×10^{-13}	–	−2.61	−2.83	−2.92	−0.24	α
^{221}U	8.409	3.68×10^{-16}	−6.18	−6.55	−6.74	−6.77	2.62	α
^{222}U	8.246	2.77×10^{-16}	−5.33	−5.65	−5.82	−5.84	5.30	α
^{223}U	8.081	1.83×10^{-17}	−4.74	−5.02	−5.17	−5.20	7.81	α
^{224}U	7.915	6.02×10^{-19}	–	−0.82	−0.89	−1.03	10.13	α
^{225}U	7.748	3.76×10^{-19}	–	−0.33	−0.36	−0.50	12.27	α
^{226}U	7.578	5.07×10^{-20}	−0.57	−0.60	−0.62	−0.63	14.24	α
^{227}U	7.406	1.68×10^{-20}	1.82	1.93	1.99	2.00	16.02	α
^{228}U	7.232	2.56×10^{-21}	2.74	2.90	2.99	3.01	17.63	α
^{229}U	7.054	7.78×10^{-22}	–	1.91	2.07	1.91	19.06	α
^{230}U	6.874	1.47×10^{-22}	6.24	6.61	6.81	6.86	20.30	α
^{231}U	6.688	3.41×10^{-23}	–	3.23	3.51	3.35	21.38	α
^{232}U	6.499	2.20×10^{-23}	9.34	9.89	10.19	10.26	22.27	α
^{233}U	6.304	3.46×10^{-24}	12.70	13.45	13.86	13.96	22.98	α
^{234}U	6.104	2.85×10^{-24}	12.89	13.65	14.07	14.17	23.51	α
^{235}U	5.901	1.62×10^{-24}	16.35	17.29	17.84	17.97	23.87	α
^{236}U	5.696	1.14×10^{-24}	–	7.47	8.11	7.99	24.05	α
^{237}U	5.491	3.82×10^{-25}	–	8.49	9.22	9.12	24.05	α
^{238}U	5.290	4.41×10^{-25}	–	9.55	10.37	10.29	23.87	α
^{239}U	5.096	1.34×10^{-25}	–	10.63	11.54	11.49	23.51	α
^{240}U	4.912	3.98×10^{-26}	–	11.71	12.72	12.69	22.97	α
^{241}U	4.740	9.21×10^{-26}	–	12.78	13.88	13.87	22.26	α
^{242}U	4.582	5.89×10^{-26}	–	13.81	15.00	15.03	21.37	α
^{243}U	4.435	4.40×10^{-26}	–	14.82	16.10	16.15	20.30	α
^{244}U	4.298	1.81×10^{-26}	–	15.81	17.17	17.26	19.05	α
^{245}U	4.165	3.88×10^{-26}	–	16.82	18.27	18.39	17.62	α
^{215}Np	9.931	1.48×10^{-17}	–	−5.45	−5.92	−5.90	−27.99	SF
^{216}Np	9.784	1.05×10^{-16}	–	−5.15	−5.59	−5.59	−23.87	SF
^{217}Np	9.636	1.89×10^{-18}	–	−4.83	−5.25	−5.26	−19.92	SF
^{218}Np	9.485	2.35×10^{-17}	–	−4.50	−4.89	−4.92	−16.16	SF
^{219}Np	9.333	3.16×10^{-19}	–	−4.17	−4.53	−4.57	−12.58	SF
^{220}Np	9.179	4.59×10^{-16}	–	−3.81	−4.14	−4.20	−9.17	SF
^{221}Np	9.023	5.03×10^{-15}	–	−3.45	−3.75	−3.81	−5.95	α
^{222}Np	8.865	4.57×10^{-14}	–	−3.07	−3.33	−3.41	−2.90	α

Table 1. *Continued.*

Nuclei	Q (MeV)	Penetration probability	$\log(T_{1/2})$				$\log(T_{sf})$	Decay modes
			Expt.	Present work	UDL	UNIV		
^{223}Np	8.706	9.03×10^{-18}	–	−2.67	−2.90	−2.99	−0.03	α
^{224}Np	8.545	7.41×10^{-19}	–	−2.27	−2.46	−2.56	2.65	α
^{225}Np	8.383	9.46×10^{-21}	–	−1.83	−1.99	−2.10	5.16	α
^{226}Np	8.219	2.65×10^{-19}	−1.46	−1.54	−1.59	−1.60	7.49	α
^{227}Np	8.053	1.74×10^{-18}	−0.29	−0.31	−0.32	−0.32	9.64	α
^{228}Np	7.884	1.68×10^{-19}	–	−0.43	−0.47	−0.61	11.62	α
^{229}Np	7.713	3.07×10^{-21}	2.38	2.52	2.60	2.62	13.41	α
^{230}Np	7.539	1.39×10^{-21}	–	0.63	0.68	0.53	15.02	α
^{231}Np	7.362	3.14×10^{-22}	–	1.20	1.30	1.14	16.46	α
^{232}Np	7.180	2.19×10^{-22}	–	1.80	1.96	1.80	17.71	α
^{233}Np	6.993	8.29×10^{-23}	–	2.46	2.67	2.51	18.79	α
^{234}Np	6.802	9.48×10^{-24}	–	3.16	3.43	3.27	19.69	α
^{235}Np	6.606	5.38×10^{-24}	–	3.90	4.24	4.08	20.41	α
^{236}Np	6.405	3.02×10^{-24}	–	4.71	5.11	4.95	20.95	α
^{237}Np	6.203	2.42×10^{-24}	13.83	14.62	15.09	15.21	21.32	α
^{238}Np	6.001	1.03×10^{-24}	–	6.44	6.99	6.85	21.50	α
^{239}Np	5.803	6.59×10^{-25}	–	7.36	7.99	7.86	21.51	α
^{240}Np	5.612	6.70×10^{-25}	–	8.29	9.00	8.89	21.34	α
^{241}Np	5.431	2.15×10^{-25}	–	9.22	10.01	9.91	20.98	α
^{242}Np	5.262	2.32×10^{-25}	–	10.13	11.00	10.92	20.46	α
^{243}Np	5.107	6.58×10^{-26}	–	11.00	11.95	11.89	19.75	α
^{244}Np	4.963	9.95×10^{-26}	–	11.84	12.86	12.82	18.86	α
^{245}Np	4.828	3.57×10^{-26}	–	12.67	13.76	13.74	17.80	α
^{220}Pu	9.770	4.29×10^{-18}	–	−4.87	−5.29	−5.30	−18.77	SF
^{221}Pu	9.620	1.95×10^{-14}	–	−4.55	−4.94	−4.96	−15.18	SF
^{222}Pu	9.468	5.47×10^{-13}	–	−4.22	−4.58	−4.61	−11.77	SF
^{223}Pu	9.314	3.27×10^{-15}	–	−3.87	−4.20	−4.25	−8.53	SF
^{224}Pu	9.159	6.35×10^{-15}	–	−3.51	−3.81	−3.87	−5.48	SF
^{225}Pu	9.002	1.97×10^{-17}	–	−3.13	−3.40	−3.48	−2.60	SF
^{226}Pu	8.843	1.61×10^{-18}	–	−2.74	−2.98	−3.06	0.09	SF
^{227}Pu	8.682	2.37×10^{-27}	–	−2.33	−2.53	−2.64	2.61	SF
^{228}Pu	8.519	3.05×10^{-19}	–	−1.91	−2.07	−2.19	4.94	α
^{229}Pu	8.355	5.48×10^{-21}	1.92	2.03	2.10	2.11	7.10	α
^{230}Pu	8.187	3.84×10^{-21}	–	−1.00	−1.09	−1.22	9.08	α
^{231}Pu	8.016	8.59×10^{-22}	–	−0.52	−0.56	−0.70	10.88	α
^{232}Pu	7.842	6.37×10^{-22}	–	0.00	0.00	−0.15	12.50	α
^{233}Pu	7.664	2.26×10^{-22}	–	0.55	0.60	0.44	13.94	α
^{234}Pu	7.480	1.64×10^{-22}	–	1.13	1.23	1.07	15.21	α
^{235}Pu	7.292	4.93×10^{-23}	–	1.76	1.91	1.75	16.29	α
^{236}Pu	7.099	3.74×10^{-23}	2.72	2.88	2.97	2.99	17.20	α
^{237}Pu	6.902	2.39×10^{-23}	–	3.14	3.41	3.24	17.93	α
^{238}Pu	6.703	1.33×10^{-23}	9.44	9.98	10.30	10.38	18.48	α
^{239}Pu	6.504	3.74×10^{-24}	–	4.67	5.07	4.91	18.85	α
^{240}Pu	6.309	4.62×10^{-24}	11.32	11.97	12.35	12.45	19.04	α
^{241}Pu	6.120	2.75×10^{-24}	–	6.29	6.83	6.68	19.05	α
^{242}Pu	5.942	1.63×10^{-24}	13.07	13.82	14.26	14.38	18.89	α
^{243}Pu	5.776	8.00×10^{-25}	–	7.88	8.56	8.43	18.55	α
^{244}Pu	5.623	6.06×10^{-25}	15.41	16.29	16.82	16.95	18.02	α
^{245}Pu	5.483	1.22×10^{-25}	–	9.36	10.16	10.05	17.32	α
^{226}Am	9.450	5.12×10^{-19}	–	−3.91	−4.25	−4.30	−7.96	SF
^{227}Am	9.295	9.32×10^{-17}	–	−3.56	−3.87	−3.93	−5.08	SF

Table 1. *Continued.*

Nuclei	Q (MeV)	Penetration probability	$\log(T_{1/2})$				$\log(T_{sf})$	Decay modes
			Expt.	Present work	UDL	UNIV		
^{228}Am	9.138	1.90×10^{-18}	–	−3.19	−3.46	−3.54	−2.38	α
^{229}Am	8.979	3.96×10^{-20}	–	−2.80	−3.04	−3.13	0.14	α
^{230}Am	8.817	9.82×10^{-21}	–	−2.40	−2.61	−2.71	2.49	α
^{231}Am	8.653	4.46×10^{-21}	–	−1.98	−2.15	−2.26	4.65	α
^{232}Am	8.486	2.91×10^{-21}	–	−1.54	−1.67	−1.79	6.64	α
^{233}Am	8.315	1.27×10^{-21}	2.28	2.41	2.49	2.51	8.45	α
^{234}Am	8.140	8.10×10^{-22}	–	−0.57	−0.62	−0.76	10.08	α
^{235}Am	7.959	4.36×10^{-22}	–	−0.05	−0.05	−0.20	11.53	α
^{236}Am	7.774	1.73×10^{-22}	2.32	2.45	2.53	2.55	12.80	α
^{237}Am	7.584	9.25×10^{-23}	–	1.12	1.22	1.05	13.89	α
^{238}Am	7.390	4.22×10^{-23}	–	1.76	1.91	1.74	14.80	α
^{239}Am	7.194	2.45×10^{-23}	–	2.43	2.64	2.47	15.54	α
^{240}Am	6.999	1.13×10^{-23}	–	3.13	3.40	3.22	16.10	α
^{241}Am	6.806	8.92×10^{-24}	10.14	10.72	11.06	11.15	16.47	α
^{242}Am	6.621	7.87×10^{-24}	–	4.57	4.96	4.79	16.67	α
^{243}Am	6.446	2.45×10^{-23}	11.37	12.02	12.45	12.51	16.69	α
^{244}Am	6.283	1.68×10^{-24}	–	5.96	6.47	6.31	16.54	α
^{245}Am	6.133	2.16×10^{-24}	–	6.61	7.18	7.03	16.20	α
^{246}Am	5.995	1.86×10^{-24}	–	7.24	7.86	7.71	15.69	α
^{247}Am	5.865	5.79×10^{-25}	–	7.84	8.51	8.37	14.99	α
^{248}Am	5.741	3.41×10^{-25}	–	8.43	9.16	9.04	14.12	α
^{249}Am	5.615	1.70×10^{-24}	–	9.06	9.84	9.73	13.07	α
^{250}Am	5.314	1.41×10^{-24}	–	10.68	11.60	11.51	11.85	α
^{233}Cm	8.948	8.54×10^{-21}	–	−2.46	−2.67	−2.76	2.31	α
^{234}Cm	8.780	5.30×10^{-21}	1.71	1.81	1.87	1.88	4.31	α
^{235}Cm	8.608	2.54×10^{-21}	–	−1.57	−1.71	−1.83	6.12	α
^{236}Cm	8.431	1.07×10^{-21}	–	−1.10	−1.19	−1.32	7.76	α
^{237}Cm	8.249	9.52×10^{-22}	–	−0.59	−0.64	−0.78	9.21	α
^{238}Cm	8.062	1.71×10^{-22}	–	−0.05	−0.05	−0.20	10.49	α
^{239}Cm	7.871	8.06×10^{-22}	–	0.53	0.58	0.42	11.59	α
^{240}Cm	7.678	8.46×10^{-23}	6.37	6.73	6.98	7.01	12.51	α
^{241}Cm	7.486	3.81×10^{-23}	–	1.77	1.92	1.75	13.25	α
^{242}Cm	7.296	4.38×10^{-23}	–	2.41	2.62	2.44	13.82	α
^{243}Cm	7.114	3.76×10^{-23}	–	3.05	3.31	3.14	14.20	α
^{244}Cm	6.941	1.38×10^{-23}	–	3.68	4.00	3.82	14.41	α
^{245}Cm	6.781	5.25×10^{-24}	11.42	12.07	12.50	12.56	14.44	α
^{246}Cm	6.634	3.19×10^{-24}	–	4.86	5.28	5.11	14.29	α
^{247}Cm	6.499	2.17×10^{-24}	–	5.41	5.87	5.70	13.96	α
^{248}Cm	6.373	1.17×10^{-24}	–	5.93	6.44	6.28	13.45	α
^{249}Cm	6.250	1.15×10^{-24}	–	6.45	7.01	6.85	12.77	α
^{250}Cm	6.127	1.21×10^{-24}	–	7.00	7.60	7.44	11.90	α
^{251}Cm	5.829	4.95×10^{-25}	–	8.41	9.13	9.00	10.86	α
^{252}Cm	5.537	8.15×10^{-25}	–	9.90	10.75	10.64	9.64	SF
^{253}Cm	5.264	4.78×10^{-25}	–	11.40	12.38	12.31	8.24	SF
^{254}Cm	5.019	1.25×10^{-25}	–	12.85	13.96	13.92	6.67	SF
^{255}Cm	4.809	5.20×10^{-26}	–	14.18	15.40	15.40	4.91	α
^{230}Bk	10.027	9.13×10^{-19}	–	−4.68	−5.08	−5.09	−12.61	SF
^{231}Bk	9.875	1.11×10^{-19}	–	−4.35	−4.72	−4.75	−9.71	SF
^{232}Bk	9.720	6.23×10^{-20}	–	−4.01	−4.36	−4.40	−7.00	SF
^{233}Bk	9.563	4.21×10^{-20}	–	−3.66	−3.97	−4.03	−4.46	SF
^{234}Bk	9.402	2.43×10^{-20}	–	−3.29	−3.57	−3.64	−2.10	α

Table 1. *Continued.*

Nuclei	Q (MeV)	Penetration probability	$\log(T_{1/2})$				$\log(T_{sf})$	Decay modes
			Expt.	Present work	UDL	UNIV		
^{235}Bk	9.238	1.26×10^{-20}	–	−2.90	−3.15	−3.23	0.08	α
^{236}Bk	9.069	6.14×10^{-21}	–	−2.49	−2.70	−2.79	2.08	α
^{237}Bk	8.895	2.62×10^{-21}	–	−2.04	−2.22	−2.33	3.90	α
^{238}Bk	8.716	1.99×10^{-21}	–	−1.58	−1.72	−1.84	5.55	α
^{239}Bk	8.533	1.05×10^{-21}	–	−1.09	−1.18	−1.31	7.01	α
^{240}Bk	8.345	4.39×10^{-22}	–	−0.56	−0.61	−0.75	8.30	α
^{241}Bk	8.155	3.77×10^{-22}	2.44	2.58	2.67	2.68	9.40	α
^{242}Bk	7.965	1.48×10^{-21}	–	0.56	0.61	0.44	10.33	α
^{243}Bk	7.779	2.78×10^{-22}	–	1.13	1.23	1.07	11.08	α
^{244}Bk	7.599	2.01×10^{-22}	–	1.71	1.86	1.69	11.65	α
^{245}Bk	7.430	6.17×10^{-23}	–	2.27	2.47	2.30	12.05	α
^{246}Bk	7.273	3.59×10^{-23}	–	2.82	3.06	2.88	12.26	α
^{247}Bk	7.128	7.69×10^{-24}	10.64	11.25	11.65	11.70	12.30	α
^{248}Bk	6.996	5.93×10^{-24}	–	3.81	4.14	3.96	12.15	α
^{249}Bk	6.872	2.33×10^{-24}	–	4.27	4.64	4.46	11.83	α
^{250}Bk	6.753	2.45×10^{-24}	–	4.73	5.14	4.96	11.33	α
^{251}Bk	6.632	3.73×10^{-24}	–	5.20	5.65	5.48	10.65	α
^{252}Bk	6.337	7.53×10^{-24}	–	6.45	7.01	6.84	9.80	α
^{253}Bk	6.047	1.67×10^{-24}	–	7.76	8.43	8.28	8.76	SF
^{254}Bk	5.777	9.36×10^{-25}	–	9.08	9.86	9.73	7.55	SF
^{255}Bk	5.534	2.55×10^{-25}	–	10.34	11.23	11.12	6.16	SF
^{230}Cf	10.607	4.92×10^{-17}	–	−5.61	−6.09	−6.06	−21.10	SF
^{231}Cf	10.460	1.50×10^{-18}	–	−5.32	−5.78	−5.76	−17.84	SF
^{232}Cf	10.312	2.88×10^{-19}	–	−5.03	−5.46	−5.45	−14.75	SF
^{233}Cf	10.160	1.88×10^{-19}	–	−4.71	−5.12	−5.13	−11.85	SF
^{234}Cf	10.007	1.19×10^{-19}	–	−4.38	−4.76	−4.79	−9.13	SF
^{235}Cf	9.849	6.13×10^{-20}	–	−4.04	−4.39	−4.43	−6.58	SF
^{236}Cf	9.688	3.66×10^{-20}	–	−3.68	−4.00	−4.06	−4.21	SF
^{237}Cf	9.523	1.66×10^{-20}	–	−3.31	−3.59	−3.66	−2.03	SF
^{238}Cf	9.352	7.42×10^{-21}	–	−2.90	−3.15	−3.24	−0.02	α
^{239}Cf	9.177	5.60×10^{-21}	1.59	1.68	1.74	1.75	1.81	α
^{240}Cf	8.996	5.26×10^{-20}	1.76	1.86	1.93	1.94	3.46	α
^{241}Cf	8.811	1.05×10^{-21}	–	−1.55	−1.68	−1.80	4.93	α
^{242}Cf	8.625	2.55×10^{-20}	2.35	2.48	2.57	2.59	6.23	α
^{243}Cf	8.438	2.13×10^{-22}		−0.52	−0.57	−0.72	7.34	α
^{244}Cf	8.254	8.47×10^{-22}	3.06	3.24	3.37	3.39	8.28	α
^{245}Cf	8.078	6.51×10^{-22}	–	0.52	0.57	0.40	9.03	α
^{246}Cf	7.911	1.41×10^{-22}	5.11	5.40	5.60	5.63	9.61	α
^{247}Cf	7.757	4.38×10^{-23}	–	1.52	1.65	1.47	10.01	α
^{248}Cf	7.615	2.45×10^{-23}	–	1.98	2.15	1.97	10.23	α
^{249}Cf	7.486	1.94×10^{-23}	10.05	10.63	11.00	11.08	10.27	α
^{250}Cf	7.365	1.11×10^{-23}	8.62	9.11	9.44	9.50	10.14	α
^{251}Cf	7.248	1.31×10^{-23}	10.45	11.05	11.44	11.52	9.82	α
^{252}Cf	7.130	1.57×10^{-22}	–	3.64	3.95	3.77	9.33	α
^{253}Cf	6.837	1.09×10^{-23}	–	4.76	5.17	4.98	8.66	α
^{254}Cf	6.550	5.96×10^{-24}	–	5.92	6.43	6.26	7.81	α
^{255}Cf	6.282	1.73×10^{-23}	–	7.08	7.69	7.53	6.78	α
^{235}Es	10.443	8.33×10^{-18}	–	−5.06	−5.49	−5.48	−13.86	SF
^{236}Es	10.289	1.64×10^{-19}	–	−4.74	−5.15	−5.16	−11.12	SF
^{237}Es	10.132	6.66×10^{-20}	–	−4.41	−4.79	−4.81	−8.57	SF
^{238}Es	9.969	3.50×10^{-20}	–	−4.06	−4.41	−4.45	−6.20	SF

Table 1. *Continued.*

Nuclei	Q (MeV)	Penetration probability	$\log(T_{1/2})$				$\log(T_{sf})$	Decay modes
			Expt.	Present work	UDL	UNIV		
^{239}Es	9.802	1.41×10^{-20}	–	−3.68	−4.00	−4.06	−4.00	SF
^{240}Es	9.630	1.01×10^{-20}	–	−3.30	−3.58	−3.65	−1.99	SF
^{241}Es	9.452	4.60×10^{-21}	0.90	0.95	0.99	0.99	−0.15	α
^{242}Es	9.271	2.48×10^{-21}	1.13	1.19	1.24	1.25	1.51	α
^{243}Es	9.087	2.36×10^{-21}	1.32	1.40	1.45	1.45	2.99	α
^{244}Es	8.903	8.92×10^{-22}	–	−1.50	−1.63	−1.76	4.29	α
^{245}Es	8.723	4.61×10^{-22}	–	−1.02	−1.11	−1.25	5.41	α
^{246}Es	8.549	3.32×10^{-21}	–	−0.54	−0.59	−0.74	6.35	α
^{247}Es	8.385	7.77×10^{-22}	–	−0.08	−0.09	−0.25	7.11	α
^{248}Es	8.234	4.24×10^{-21}	–	0.36	0.39	0.22	7.70	α
^{249}Es	8.095	9.43×10^{-23}	–	0.76	0.83	0.67	8.11	α
^{250}Es	7.968	1.48×10^{-23}	–	1.15	1.25	1.08	8.33	α
^{251}Es	7.850	3.48×10^{-23}	–	1.52	1.65	1.47	8.38	α
^{252}Es	7.736	6.21×10^{-23}	7.61	8.05	8.33	8.39	8.26	α
^{253}Es	7.621	6.08×10^{-23}	6.25	6.61	6.84	6.89	7.95	α
^{254}Es	7.330	3.81×10^{-23}	7.38	7.80	8.08	8.13	7.46	α
^{255}Es	7.046	2.01×10^{-23}	–	4.31	4.68	4.49	6.80	α
^{256}Es	6.781	6.67×10^{-24}	–	5.35	5.81	5.62	5.96	α
^{257}Es	6.543	3.00×10^{-24}	–	6.33	6.87	6.69	4.94	α
^{258}Es	6.341	7.35×10^{-24}	–	7.20	7.82	7.65	3.74	α
^{259}Es	6.177	3.58×10^{-25}	–	7.95	8.63	8.46	2.36	SF
^{260}Es	6.050	1.55×10^{-25}	–	8.54	9.27	9.11	0.80	SF
^{235}Fm	11.020	5.56×10^{-17}	–	−5.95	−6.46	−6.40	−21.74	SF
^{236}Fm	10.873	8.82×10^{-19}	–	−5.66	−6.15	−6.11	−18.64	SF
^{237}Fm	10.723	3.76×10^{-19}	–	−5.38	−5.84	−5.81	−15.72	SF
^{238}Fm	10.568	1.62×10^{-19}	–	−5.06	−5.50	−5.50	−12.98	SF
^{239}Fm	10.409	9.04×10^{-20}	–	−4.74	−5.15	−5.16	−10.42	SF
^{240}Fm	10.245	4.70×10^{-20}	–	−4.40	−4.78	−4.80	−8.04	SF
^{241}Fm	10.076	3.33×10^{-20}	–	−4.04	−4.39	−4.42	−5.84	SF
^{242}Fm	9.901	1.58×10^{-20}	–	−3.66	−3.97	−4.02	−3.82	SF
^{243}Fm	9.723	7.62×10^{-21}	–	−3.25	−3.53	−3.60	−1.97	α
^{244}Fm	9.542	7.26×10^{-21}	–	−2.83	−3.07	−3.15	−0.31	α
^{245}Fm	9.361	2.74×10^{-21}	–	−2.38	−2.59	−2.69	1.18	α
^{246}Fm	9.184	3.28×10^{-19}	–	−1.94	−2.11	−2.23	2.48	α
^{247}Fm	9.013	1.59×10^{-21}	1.49	1.58	1.63	1.64	3.61	α
^{248}Fm	8.852	7.13×10^{-20}	1.54	1.63	1.69	1.70	4.56	α
^{249}Fm	8.704	4.20×10^{-22}	–	−0.69	−0.75	−0.89	5.33	α
^{250}Fm	8.568	7.14×10^{-22}	3.26	3.45	3.59	3.61	5.93	α
^{251}Fm	8.444	4.59×10^{-22}	–	0.04	0.04	−0.12	6.34	α
^{252}Fm	8.328	1.53×10^{-22}	–	0.36	0.39	0.23	6.58	α
^{253}Fm	8.217	1.93×10^{-22}	–	0.69	0.75	0.58	6.63	α
^{254}Fm	8.105	3.22×10^{-22}	4.07	4.30	4.48	4.51	6.51	α
^{255}Fm	7.817	2.36×10^{-22}	4.86	5.14	5.35	5.38	6.21	α
^{256}Fm	7.535	1.02×10^{-22}	–	2.89	3.14	2.95	5.73	α
^{257}Fm	7.272	5.64×10^{-23}	–	3.82	4.15	3.96	5.08	α
^{258}Fm	7.037	4.61×10^{-22}	–	4.70	5.10	4.91	4.24	α
^{259}Fm	6.838	2.48×10^{-24}	–	5.48	5.95	5.76	3.23	SF
^{260}Fm	6.676	7.47×10^{-25}	–	6.13	6.66	6.48	2.04	SF
^{240}Md	10.841	3.59×10^{-17}	–	−5.38	−5.84	−5.81	−14.69	SF
^{241}Md	10.681	4.55×10^{-19}	–	−5.06	−5.49	−5.48	−12.12	SF
^{242}Md	10.514	2.65×10^{-19}	–	−4.72	−5.13	−5.13	−9.74	SF

Table 1. *Continued.*

Nuclei	Q (MeV)	Penetration probability	$\log(T_{1/2})$				$\log(T_{sf})$	Decay modes
			Expt.	Present work	UDL	UNIV		
^{243}Md	10.343	1.66×10^{-19}	–	−4.36	−4.74	−4.76	−7.53	SF
^{244}Md	10.168	8.10×10^{-20}	–	−3.99	−4.33	−4.37	−5.50	SF
^{245}Md	9.990	9.97×10^{-20}	−3.05	−3.22	−3.36	−3.38	−3.65	SF
^{246}Md	9.812	5.86×10^{-20}	–	−3.20	−3.47	−3.54	−1.97	α
^{247}Md	9.638	1.07×10^{-20}	–	−2.79	−3.03	−3.11	−0.48	α
^{248}Md	9.470	1.20×10^{-20}	–	−2.38	−2.59	−2.69	0.83	α
^{249}Md	9.312	5.81×10^{-21}	–	−2.00	−2.17	−2.28	1.97	α
^{250}Md	9.166	2.88×10^{-21}	–	−1.63	−1.77	−1.90	2.93	α
^{251}Md	9.033	8.62×10^{-21}	–	−1.29	−1.40	−1.54	3.71	α
^{252}Md	8.912	2.29×10^{-22}	–	−0.98	−1.06	−1.20	4.31	α
^{253}Md	8.799	3.24×10^{-21}	–	−0.68	−0.74	−0.88	4.73	α
^{254}Md	8.691	2.04×10^{-21}	–	−0.39	−0.42	−0.57	4.97	α
^{255}Md	8.581	1.61×10^{-21}	–	−0.08	−0.09	−0.25	5.03	α
^{256}Md	8.296	1.32×10^{-21}	–	0.76	0.82	0.65	4.92	α
^{257}Md	8.017	4.72×10^{-22}	–	1.62	1.76	1.58	4.63	α
^{258}Md	7.756	1.44×10^{-22}	0.65	0.69	0.72	0.72	4.15	α
^{259}Md	7.524	6.12×10^{-23}	–	3.26	3.54	3.35	3.51	α
^{260}Md	7.327	5.95×10^{-24}	–	3.97	4.31	4.11	2.68	SF
^{245}No	10.605	1.36×10^{-17}	–	−4.66	−5.06	−5.07	−9.05	SF
^{246}No	10.430	4.67×10^{-19}	–	−4.30	−4.67	−4.69	−7.02	α
^{247}No	10.255	2.72×10^{-19}	–	−3.92	−4.26	−4.30	−5.16	α
^{248}No	10.083	4.99×10^{-20}	–	−3.55	−3.85	−3.91	−3.48	α
^{249}No	9.919	6.38×10^{-20}	–	−3.18	−3.45	−3.52	−1.98	α
^{250}No	9.764	5.05×10^{-21}	–	−2.83	−3.07	−3.15	−0.66	α
^{251}No	9.621	1.46×10^{-20}	–	−2.49	−2.70	−2.80	0.49	α
^{252}No	9.490	1.00×10^{-20}	0.39	0.41	0.43	0.43	1.45	α
^{253}No	9.372	2.65×10^{-21}	–	−1.89	−2.05	−2.17	2.24	α
^{254}No	9.262	3.06×10^{-21}	1.71	1.81	1.88	1.89	2.84	α
^{255}No	9.156	7.37×10^{-21}	–	−1.35	−1.47	−1.60	3.27	α
^{256}No	9.049	3.24×10^{-19}	–	−1.08	−1.17	−1.31	3.52	α
^{257}No	8.766	8.10×10^{-21}	1.39	1.47	1.53	1.54	3.59	α
^{258}No	8.490	4.65×10^{-20}	3.54	3.74	3.89	3.92	3.48	α
^{259}No	8.232	7.31×10^{-22}	–	1.27	1.38	1.19	3.20	α
^{260}No	8.003	1.45×10^{-22}	–	1.99	2.16	1.97	2.73	α
^{261}No	7.808	5.74×10^{-23}	–	2.62	2.85	2.65	2.09	SF
^{262}No	7.651	7.42×10^{-24}	–	3.15	3.42	3.22	1.27	SF
^{263}No	7.531	3.23×10^{-24}	–	3.56	3.87	3.66	0.27	SF
^{264}No	7.443	1.10×10^{-24}	–	3.87	4.20	3.99	−0.91	SF
^{265}No	7.379	1.28×10^{-24}	–	4.08	4.43	4.23	−2.26	SF
^{245}Lr	11.199	1.08×10^{-16}	–	−5.60	−6.08	−6.04	−15.04	SF
^{246}Lr	11.030	1.40×10^{-18}	–	−5.28	−5.73	−5.70	−12.64	SF
^{247}Lr	10.858	1.23×10^{-18}	–	−4.94	−5.36	−5.35	−10.41	SF
^{248}Lr	10.686	6.95×10^{-19}	–	−4.59	−4.98	−4.99	−8.37	SF
^{249}Lr	10.518	1.22×10^{-19}	–	−4.24	−4.60	−4.63	−6.50	SF
^{250}Lr	10.356	4.45×10^{-20}	–	−3.89	−4.23	−4.27	−4.82	SF
^{251}Lr	10.204	5.22×10^{-20}	–	−3.56	−3.87	−3.93	−3.31	α
^{252}Lr	10.063	2.86×10^{-20}	–	−3.26	−3.54	−3.60	−1.98	α
^{253}Lr	9.936	8.06×10^{-21}	–	−2.97	−3.23	−3.30	−0.83	α
^{254}Lr	9.820	4.61×10^{-21}	–	−2.71	−2.94	−3.03	0.14	α
^{255}Lr	9.713	2.29×10^{-21}	–	−2.46	−2.67	−2.77	0.93	α

Table 1. *Continued.*

Nuclei	Q (MeV)	Penetration probability	$\log(T_{1/2})$				$\log(T_{sf})$	Decay modes
			Expt.	Present work	UDL	UNIV		
^{256}Lr	9.610	6.36×10^{-19}	–	−2.22	−2.41	−2.51	1.55	α
^{257}Lr	9.506	2.29×10^{-20}	–	−1.97	−2.14	−2.25	1.98	α
^{258}Lr	9.226	1.97×10^{-19}	–	−1.25	−1.36	−1.49	2.24	α
^{259}Lr	8.952	7.86×10^{-21}	–	−0.52	−0.56	−0.72	2.32	α
^{260}Lr	8.697	1.55×10^{-21}	–	0.19	0.21	0.05	2.22	α
^{261}Lr	8.469	3.02×10^{-22}	–	0.86	0.93	0.75	1.94	α
^{262}Lr	8.277	1.30×10^{-22}	–	1.44	1.56	1.37	1.48	α
^{263}Lr	8.123	1.54×10^{-23}	–	1.92	2.08	1.89	0.85	SF
^{264}Lr	8.006	7.81×10^{-24}	–	2.28	2.48	2.28	0.03	SF
^{265}Lr	7.920	2.35×10^{-24}	–	2.55	2.77	2.57	−0.96	SF

(MeV), M_α is the mass of α-particle and M_d is the mass of the daughter nucleus. R_{in} and R_{out} are the inner and outer classical turning points determined by the relation

$$V(R = R_{in}, R_{out}) = Q_\alpha. \quad (5)$$

Total potential ($V(R)$) is considered as the sum of the Coulomb, the nuclear and the centrifugal potentials:

$$V(R) = V_C(R) + V_N(R) + V_{cf}(R). \quad (6)$$

For the α–daughter nucleus interaction, we adopt the Coulomb potential given by

$$V_C(R) = \begin{cases} \dfrac{2Ze^2}{R}, & R > R_m, \\ \dfrac{Ze^2}{R_m}\left(3 - \dfrac{R^2}{R_m^2}\right), & R \le R_m, \end{cases} \quad (7)$$

where the parameters are given by Li *et al* [11] and Denisov and Ikezoe [12]. R_m is the effective radius of the nuclear part of the α–nucleus potential and it is given by the following equation:

$$R_m = 1.5268 + R_0. \quad (8)$$

Here R_0 is the radius of the nucleus interacting with the α-particle:

$$R_0 = R_p\left(1 + \frac{3.0909}{R_p^2}\right) + 0.12430\left(\frac{A - 2Z}{A} - \frac{0.4A}{A + 200}\right), \quad (9)$$

where R_p is the proton radius defined in ref. [13],

$$R_p = 1.2A^{1/3}\left[1 + \frac{1.646}{A} - \frac{0.191(A - 2Z)}{A}\right], \quad (10)$$

where A and Z are the mass and charge numbers of the daughter nucleus, respectively. For the nuclear part, the Woods–Saxon potential is adopted:

$$V_N(R) = \frac{V_0}{1 + \exp((R - R_m)/a_0)}, \quad (11)$$

a_0 is the diffuseness parameter taken to be 0.49290 fm and V_0 (MeV) is the nuclear potential strength which is empirically given by the following proposed formula [12,14]:

$$V_0 = -\left[47 - \frac{0.46Z}{A^{1/3}} + \frac{38(A - 2Z)}{A}\right]. \quad (12)$$

For the centrifugal potential, the Langer-modified centrifugal barrier is adopted from ref. [15]:

$$V_{cf} = \frac{h^2(l + (1/2))^2}{8\pi^2 \times \mu R^2}, \quad (13)$$

where l is the angular momentum quantum number carried by the emitted α-particle.

3. Results and discussion

The energy released (Q_α) during the α decay between the ground state of the parent nuclei and the ground state of the daughter nuclei is calculated using the procedure explained in our previous work [14–16]. In this work, we have used this experimental mass excess data [17]. Some of the experimental mass excess values are not available. For those nuclei, where experimental mass excess was unavailable, we have used recent theoretical values [17,18]. The mass excess data are taken from [18,19].

Variations of logarithmic half-lives with the mass number of the parent nuclei for the studied actinides of atomic number region $89 < Z < 103$ are shown in figure 1. In this figure, we have plotted the logarithmic fission half-lives along with the α decay half-lives. The spontaneous fission half-lives are computed using the semiempirical relation given by Xu *et al* [20]. The

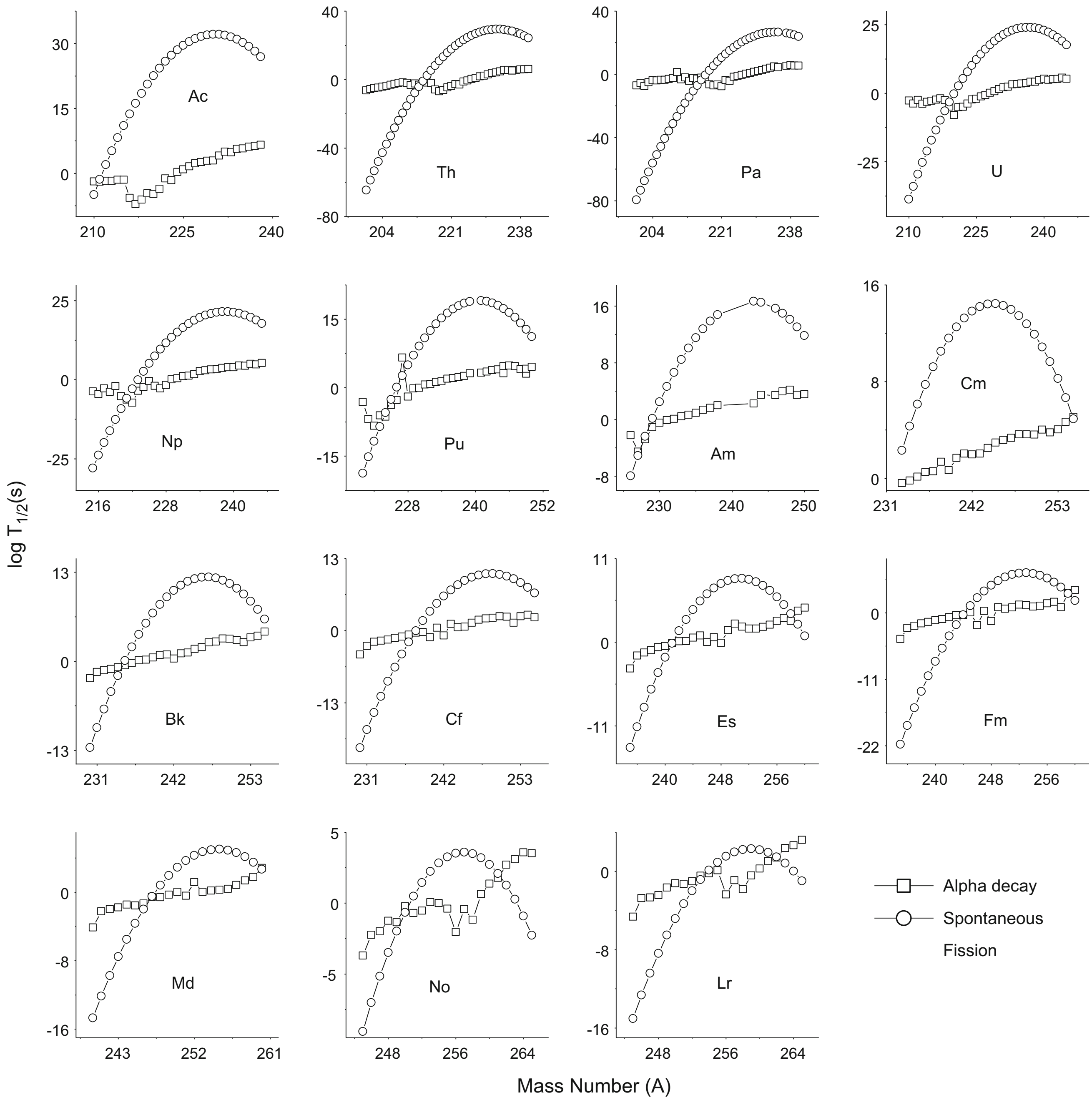

Figure 1. Variation of the calculated logarithmic half-lives for α decay and spontaneous fission with the mass number of parent nuclei.

variation of the computed spontaneous fission half-lives with mass number is found to be Gaussian. The mass density distribution of the parent nucleus is the standard Gaussian form [21,22]. The distribution of total neutron emission numbers is Gaussian-like in spontaneous fission with centres at the average neutron multiplicity [23,24]. The total kinetic energy distributions are almost Gaussian in shape for the spontaneous fission in the actinide nuclei. This may be the reason for the Gaussian variation of the spontaneous fission half-lives with mass number. To compare the results of this work with those of the experiments available in the literature, we have also calculated the α decay half-lives using a different formula available in the literature such as universal decay law (UDL) [25] and UNIVersal (UNIV) [26]. To verify the Geiger–Nuttall law for actinides, we have also plotted the logarithmic half-lives as a function of the inverse square root of the energy released, and it is shown in figure 2. From this figure, it is observed that the variation of logarithmic half-lives with the inverse

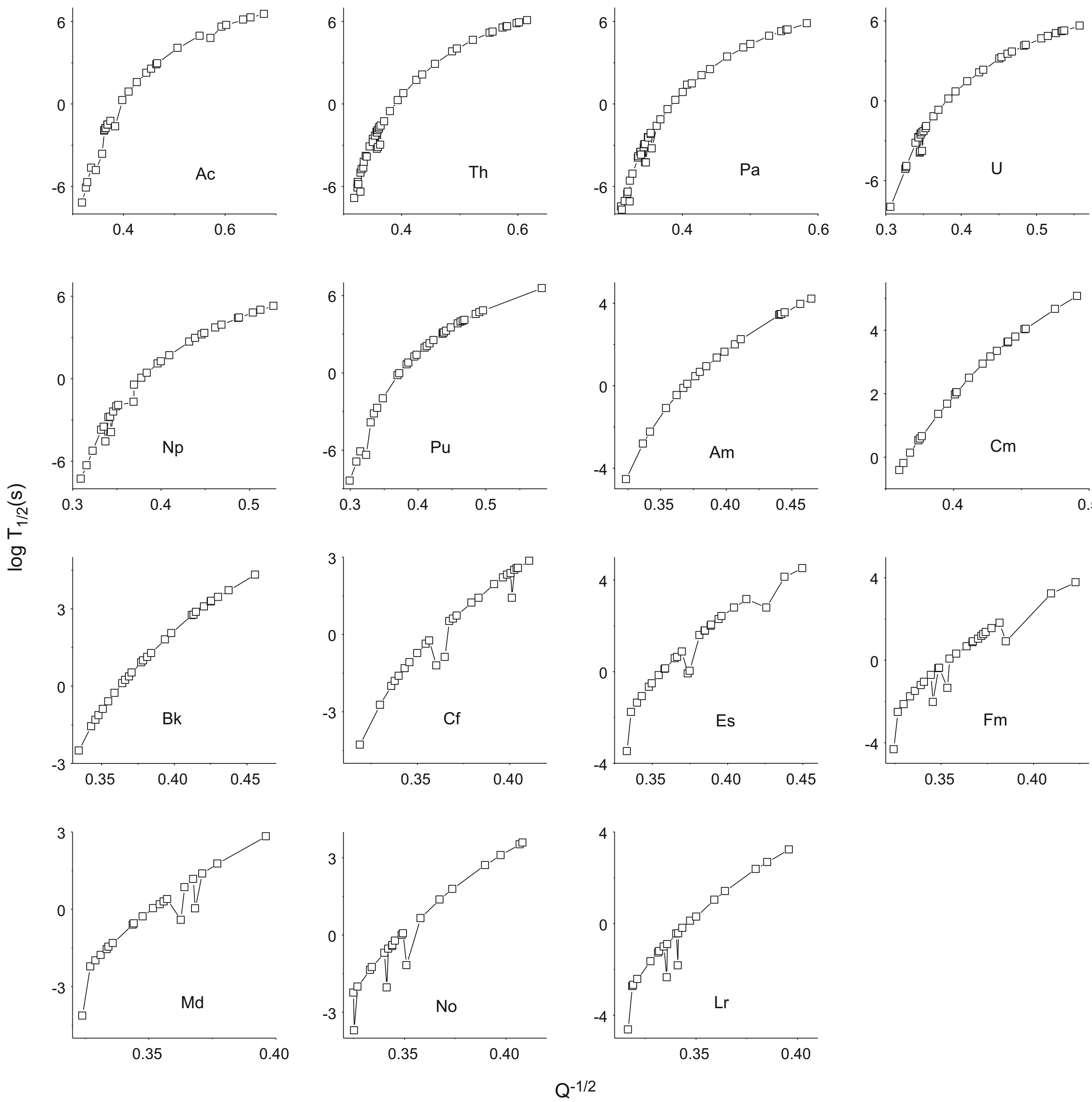

Figure 2. Variation of the calculated logarithmic half-lives with inverse square root of the energy released.

square root of the energy released ($1/\sqrt{Q}$) is not linear. Table 1 presents the logarithmic α decay half-lives calculated using the present model along with that of the values produced by the UDL [25] and UNIV [26]. To identify the dominant decay mode, we have also presented the spontaneous fission half-lives in table 1. We have studied the competition between the spontaneous fission and α decay. The decay mode having shorter half-lives is considered as the dominant decay mode. We have identified the dominant decay mode among the studied isotopes of actinides.

The decay mode with shorter half-lives is considered as the dominant decay mode. From a comparison of the spontaneous fission half-lives with that of the α decay, it is found that for the nuclei ^{210}Ac, spontaneous fission half-lives are shorter than the α decay half-lives. Hence the nuclei ^{210}Ac undergo decay through spontaneous fission. For the nuclei $^{211-238}$Ac, α decay half-lives are shorter than the spontaneous fission half-lives. Hence, the nuclei $^{211-238}$Ac undergo decay through α emission. For the nuclei $^{200-213}$Th, α decay half-lives are larger than the spontaneous fission half-lives. Hence the

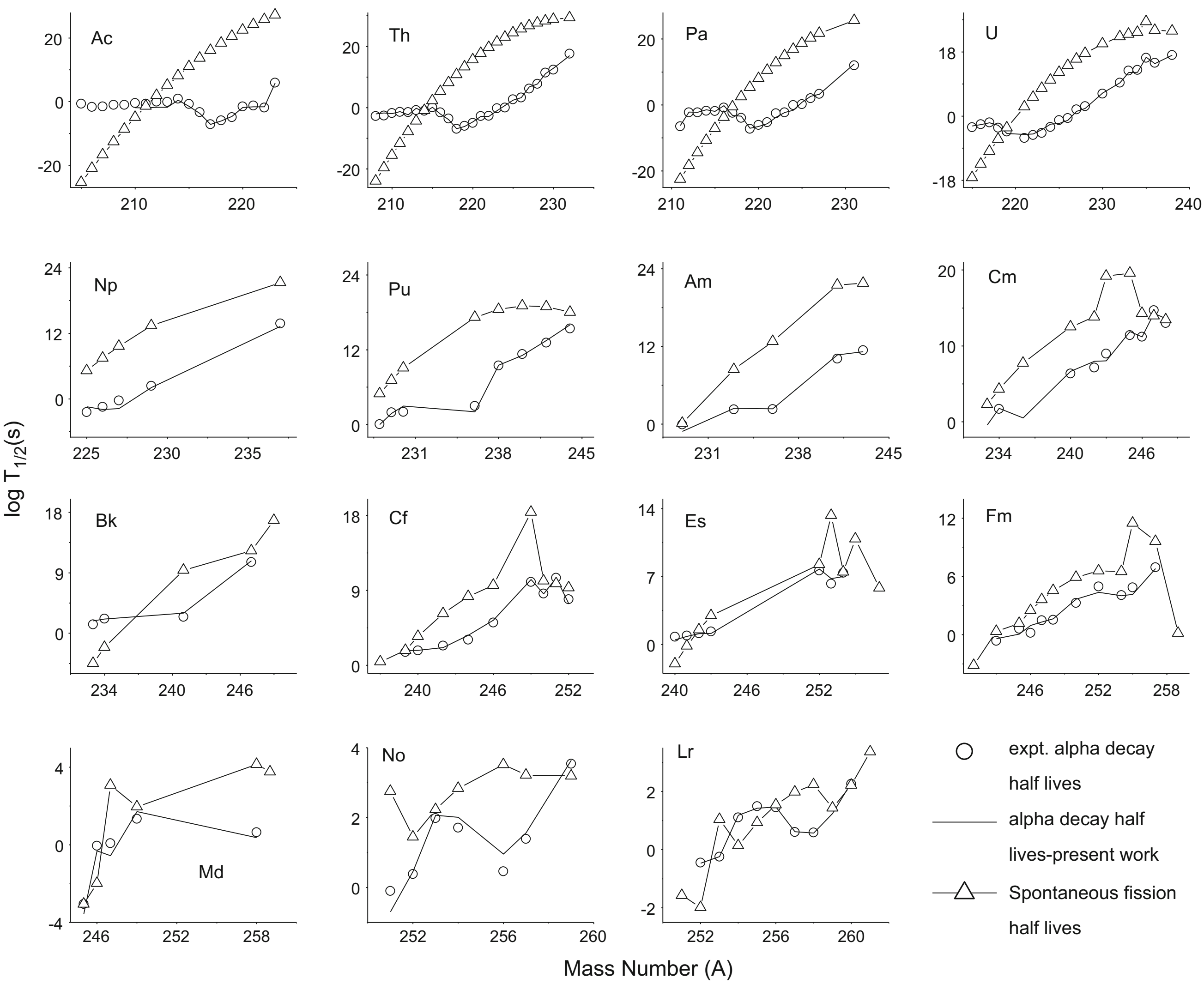

Figure 3. Comparison of this work with experiments in the literature.

nuclei $^{200-213}$Th undergo decay through spontaneous fission. For the nuclei $^{214-236}$Th, α decay half-lives are shorter than the spontaneous fission half-lives. Hence the nuclei $^{214-236}$Th undergo decay through α emission. For the actinide element Pa, the isotopes $^{200-216}$Pa decay through spontaneous fission and the isotopes $^{217-240}$Pa decay through α emission. Similarly, for the actinide element uranium, the isotopes $^{210-218}$U decay through spontaneous fission and the isotopes $^{219-245}$U decay through α emission. For the actinide element Np, the isotopes $^{215-220}$Np decay through spontaneous fission and the isotopes $^{221-245}$Np decay through α emission. For the actinide element Pu, the isotopes $^{220-227}$Pu decay through spontaneous fission and the isotopes $^{228-245}$Pu decay through α emission. For the actinide element Am, the isotopes $^{226-227}$Am decay through spontaneous fission and the isotopes $^{228-250}$Am decay through α emission.

For the actinide element Cm, the isotopes $^{252-254}$Cm decay through spontaneous fission and the isotopes $^{233-251,255}$Cm decay through α emission. For the actinide element Bk, the isotopes $^{230-233,253-255}$Bk decay through spontaneous fission and the isotopes $^{234-252}$Bk decay through α emission. For the actinide element Cf, the isotopes $^{230-237}$Cf decay through spontaneous fission and the isotopes $^{238-255}$Cf decay through α emission. For the actinide element Es, the isotopes $^{235-240,259-260}$Es decay through spontaneous fission and the isotopes $^{241-258}$Es decay through α emission. For the actinide element Fm, the isotopes $^{235-242,259-260}$Fm decay through spontaneous fission and the isotopes $^{243-258}$Fm decay through α emission. For the actinide element Md, the isotopes $^{240-245,260}$Md decay through spontaneous fission and the isotopes $^{246-259}$Md decay through α emission. For the actinide element No, the isotopes $^{245,261-265}$No decay through spontaneous fission and the isotopes $^{246-260}$No decay through α emission. For the actinide element Lr, the isotopes $^{245-250,263-265}$Lr decay through spontaneous fission and the isotopes $^{251-262}$Lr decay through α emission. The highlighted decay modes for isotopes of actinides are as shown in table 1. To validate this work, we have also compared the values produced by the present model with those of the experiments [27] available in the literature (figure 3). This comparison is also included in table 1. A comparison of the calculated logarithmic half-lives with the experiments is also shown in figure 2.

4. Conclusion

We have studied the α decay properties of actinides of atomic number $89 < Z < 103$. Geiger–Nuttall plots are presented for actinides. The dominant decay mode for each actinide nuclei is also identified.

References

[1] S Dahmardeh, S A Alavi and V Dehghani, *Nucl. Phys. A* **963**, 68 (2017)
[2] H B Yang, L Ma, Z Y Zhang, C L Yang and Z G Gan, *Phys Lett. B* **777**, 212 (2018)
[3] N Sowmya and H C Manjunatha, *Bull. J. Phys.* **46**, 16 (2019)
[4] S Mukherjee, N L Singh and J Rama Rao, *Pramana – J. Phys.* **49**(**1**), 311 (1993)
[5] H C Manjunatha, K N Sridhar and N Sowmya, *Phys. Rev. C* **98**, 024308 (2018)
[6] N Maroufi, V Dehghani and S A Alavi, *Nucl. Phys. A* **983**, 77 (2019)
[7] W J Weber, R C Ewing and A Meldrum, *J. Nucl. Mater.* **250**, 14 (1997)
[8] M Mirea, R Budaca and A Sandulescu, *Anal. Phys.* **380**, 154 (2017)
[9] H C Manjunatha and N Sowmya, *Nucl. Phys. A* **969**, 28 (2018)
[10] A O Silişteanu and A I Budaca, *At. Data Nucl. Data Tables* **98**, 1096 (2012)
[11] L L Li, S G Zhou, E G Zhao and W Scheid, *Int. J. Mod. Phys. E* **19**, 359 (2010)
[12] V Y Denisov and H Ikezoe, *Phys. Rev. C* **72**, 064613 (2005)
[13] B N Pomorska and K Pomorski, *Z. Phys. A* **348**, 169 (1994)
[14] M Ismail, A Y Ellithi, A E Depsy and O A Mohamedien, *Int. J. Mod. Phys. E* **25**, 1650069 (2016)
M Ismail, A Y Ellithi, M M Botros and A Adel, *Phys. Rev. C* **81**, 024602 (2010)
[15] H C Manjunatha, *Int. J. Mod. Phys. E* **25**(**11**), 1650100 (2016); *Int. J Mod. Phys. E* **25**(**9**), 1650074 (2016)
[16] H C Manjunatha, *Nucl. Phys. A* **945**, 42 (2016)
[17] https://www-nds.iaea.org/RIPL-3/
[18] M Kowal, P Jachimowicz and J Skalski, arXiv:1203.5013
[19] H C Manjunatha, B M Chandrika and L Seenappa, *Mod. Phys. Lett. A* **31**(**28**), 1650162 (2016)
[20] C Xu, Z Ren and Y Guo, *Phys. Rev. C* **78**, 044329 (2008)
[21] C Xu and Z Ren, *Nucl. Phys. A* **753**, 174 (2005); *Nucl. Phys. A* **760**, 303 (2005)
[22] G R Satchler and W G Love, *Phys. Rep.* **55**, 183 (1979)
[23] J Terrell, *Phys. Rev.* **108**, 784 (1957)
[24] H C Manjunatha and N Sowmya, *Pramana – J. Phys.* **90**: 62 (2018)
[25] C Qi, F R Xu, R J Liotta and R Wyss, *Phys. Rev. Lett.* **103**, 072501 (2009)
[26] D N Poenaru, R A Gherghescu and W Greiner, *Phys. Rev. C* **83**, 014601 (2011)
[27] https://www-nds.iaea.org/relnsd/vcharthtml/VChartHTML.html